FABRICATION AND CHARACTERIZATION OF TRANSITION METAL HYDRIDES FOR RADIATION SHIELDING IN TOKAMAK DEVICES

National Laboratory **Principal Investigator**	Los Alamos National Laboratory (LANL) Dr. Caitlin Kohnert (formerly Caitlin Taylor) caitlin@lanl.gov
Company **Principal Investigator**	Tokamak Energy Dr. Tom Davis tom.davis@tokamakenergy.co.uk
Award	INFUSE 2022
Period of Performance	10/08/2021 – 04/08/2023
Report Prepared by	Dr. Tyler Smith tylers@lanl.gov
Final Report Submission Date	

1 Technical Overview

1.1 Problem Statement

Describe the Tokamak Energy challenges this program is meant to address. Should be adapted from original application, noting any departures / evolutions from that original application.

Tokamak Energy is a privately funded fusion energy company, which seeks to deliver fusion energy to the electrical grid by the 2030s. Tokamak Energy's approach is based on the merging of two primary technology paths – the first being the Spherical Tokamak (ST) geometry and the second being the use of High Temperature Superconducting (HTS) tape to deliver the necessary magnetic field strengths to confine the plasma.

Radiation shielding materials are required to protect the system components during operation. Transition metal-hydrides have been identified as a key material to achieve this protection. However, additional work is required to optimize powder metallurgy fabrication for the different metal hydrides under consideration for radiation shielding. This project aim is to demonstrate successful fabrication of the most promising candidate metal hydride, hafnium hydride, through the powder metallurgy process. Microstructural and thermal property characterization of the hydride has been performed to assess its feasibility in a reactor environment. The project did not deviate from the original INFUSE application except for no neutron scattering experiments were conducted because of the beamline downtime during the timeframe.

1.2 Work Scope

Describe the approach used to achieve the project goals, including the capabilities at the national laboratory or partner facility, as well as the capabilities at Tokamak Energy and its subcontractors on this award. Can be informed / adapted from original application, noting departures / evolutions

The scope of this work is focused on the utilization of powder metallurgy and hydride expertise maintained by LANL to fabricate high density, high hydride concentration hafnium hydride powder metallurgy samples, and investigate the thermophysical performance for radiation shielding. This project aims demonstrate the fabrication of the most promising candidate metal hydride through the powder metallurgy process.

Hafnium hydride was selected as the most promising metal hydride candidate because of its superior neutron absorption and moderating properties [1]. This is based on a prior detailed neutronics study of central column radiation shielding and materials scoping exercise.

The tasks of the project consisted of the following:

1. Material Fabrication
2. Assessment of the Microstructural and Thermal Properties
3. Completion of the Final Report
4. Send high density, high hydride concentrated HfH_x samples to Tokamak Energy for future irradiation testing and analysis.

1.3 Results

Describe the tasks accomplished, results obtained, key deliverables, lessons learned. Do not include proprietary information.

The results from this proposal can be separated into two categories: (1) the fabrication and development of the dense hafnium hydride, and (2) the thermal and mechanical properties of the densest hafnium hydride. The lessons learned are discussed here.

To eliminate contamination and impurity effects on the hydride, the manufacturing route for this study started with pure hafnium feedstock and direct hydriding. Then the direct HfHx was crushed, sieved, and then underwent powder metallurgy manufacturing process. The impact of feedstock powder of HfH was out of scope. The fabrication process was as follows:

1. Fabrication of the metal hydrides began with a hafnium feedstock (99.9% pure, excluding Zr. 2.96% Zr) obtained from Kurt J. Leskar, that was charged with hydrogen using hydriding methods developed at LANL.
2. The resultant hydrided feedstock of $HfH_{1.5}$ is shown in Figure 1. Cracking is to be expected as the process was not optimized for non-cracked hydrides.
3. This hydrided feedstock was then sieved and pressed to a green density of ~71% before undergoing proceeding sintering tests. In this report, “density” refers to “percent of theoretical density” and is given by the expression in Equation 1.

$$\text{density} = \frac{\text{measured density}}{\text{theoretical density}} \times 100 \quad (1)$$

Impurity	Wt. ppm
Fe	150
O	250
Al, C, Co, Cr, C, H, Mn, Mo, Nb, Ni, Pb, Si, Sn, Ta, Ti, U, V, W, N	<50 each

Figure 1. (a) Hf feedstock composition (b) Hydrided hafnium feedstock ($HfH_{1.52}$)

A systematic series of hydride/sintering tests were conducted in a gettered Ar/6%H environment on the green density hydride feedstock pellets to produce high density, high hydrogen concentration hafnium hydride samples. Solid machined Hf samples, referred to as "direct hydride" samples were included in the first few hydriding runs for comparison. Samples were placed on top of a molybdenum plate which was then placed on a bed of tabular alumina inside an alumina crucible. A zirconium crucible was placed over the samples to help further getter the Ar/6%H atmosphere. The summary of these results is given in Table 1. The distinction between Sintering A-E is the sintering temperature.

The theoretical densities were calculated from lattice parameters measured by diffraction that was found within the literature. The theoretical densities used to calculate densities in Table 1.

Table 1. Summary of HfH_x density, phase, and H/Hf ratio from each sintering run as compared to the Green Pellet hydrided feedstock. H/Hf ratio was determined by LECO analysis.

Sample	**Theoretical Density (g/cm^3)** [2, 3, 4, 5]	**Density**	**Phase**	**H/Hf**
Green Pellet	11.47	70.95%	Epsilon	1.52
Sintering A	11.47	71.80%	Epsilon	1.48
Sintering B	11.52	80.79%	Delta + Epsilon	1.76
Sintering C	11.38	84.08%	Epsilon	1.83
Sintering D	11.38	90.91%	Epsilon	1.89
Sintering E for Irradiation	11.38	90.46%	Epsilon	2.0

X-ray diffraction (XRD) was performed on representative samples from each sintering run to determine the phase of the metal hydrides. The results are summarized in Figure 2. All samples were in the epsilon phase except for the sample B, that yielded a mixed phase of both epsilon (tetragonal) and delta (cubic) phases. This may have been partially due to the hydriding procedure straddling the phase boundary, and partially due to the new furnace setup having some residual oxidation contamination. The white powder, shown in Figure 3 (b), was analyzed by XRD and proved to be ZrO_2. A new O_2 monitor was installed on ensuing sintering runs to ensure that the furnace environment was free of contamination.

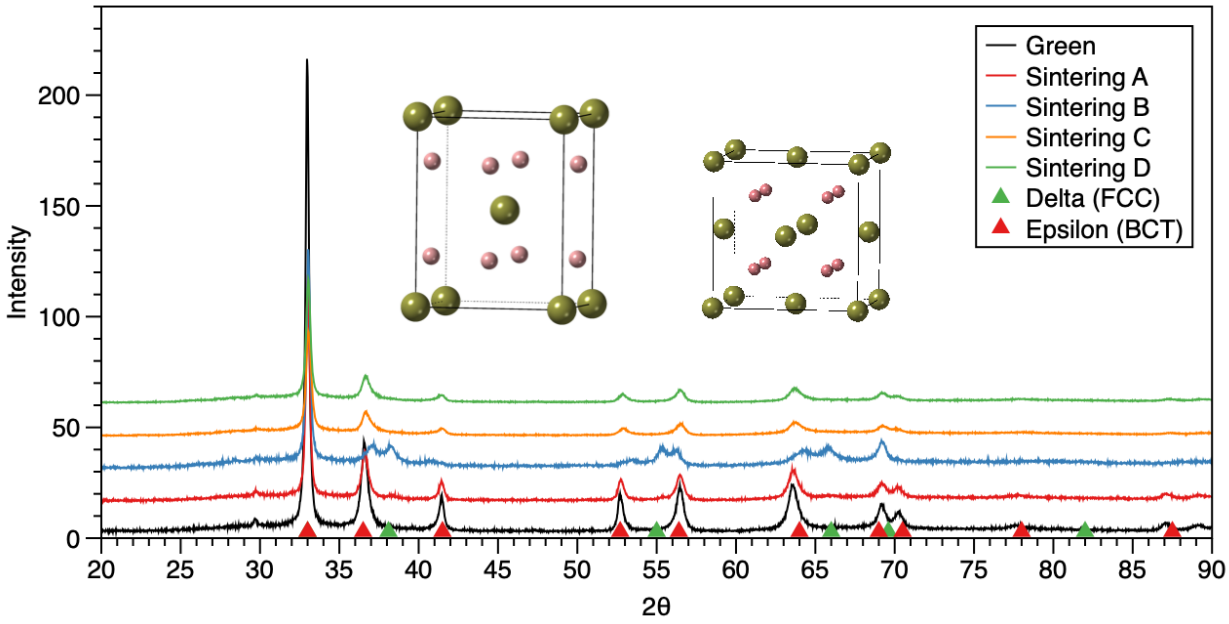

Figure 2. XRD patterns of each sintering run compared to the hydrided feedstock. The hydrogen atoms are shown in pink and the hafnium atoms are shown in green within the crystal structures.

The first sintering run utilized a low temperature furnace that resides in the same glovebox that the green pellets were fabricated. The XRD results for a maximum sintering temperature of the furnace, called Sintering A, shown in Figure 2, revealed that the samples remained in the epsilon (tetragonal) phase at $HfH_{1.48}$. The density calculations and SEM image (Figure 4) show that uniform sintering and hydriding were achieved with an approximate increase of 1% density up to 71.80%. It can also be observed in Figure 3a that cracking is not as prevalent in the powder metallurgy samples compared to the direct-hydrided samples. This advantage in powder metallurgy can be attributed to the sample's porosity serving as a relief mechanism during hydriding when the sample experiences a volume expansion.

To increase H/Hf ratio and density, a new tube furnace capable of temperatures up to a high temperature was configured for this process. First, maximum sintering temperature was increased to higher temperature than Sintering A, yielding an increase in hydrogen concentration ($HfH_{1.76}$) and an approximate 9% increase in density (80.79% dense). However, a mixed phase of delta and epsilon hydride (Sintering B) formed in the sample that may not be ideal for fusion applications.

Raising the sintering temperature to Sintering C values increased the density by another ~3% (84.08%) and the H/Hf ratio by 0.07 ($HfH_{1.83}$). XRD results revealed that the samples once again returned to the epsilon hydride phase and the oxygen contamination was no longer a factor. Various samples were fabricated in dimensions needed for thermophysical property measurements at this temperature to see how sample size affects hydriding. Some microcracking did occur in the larger (5mm x 5mm and 5mm x 2.5mm) samples.

Finally, at a sintering temperature Sintering D, samples prepared for thermophysical property measurements reached $HfH_{1.89}$ with an approximate 6% increase in density (90.91%). XRD revealed that the samples remained in the epsilon phase and thermophysical measurements were able to commence. A second and third round of the same parameters as Sintering D runs

were performed for samples fabricated for irradiation testing. These samples yielded epsilon phase HfH_2, as confirmed in Figure 4d and 4e, with a density of 90.46%. We refer to these samples as Sintering E.

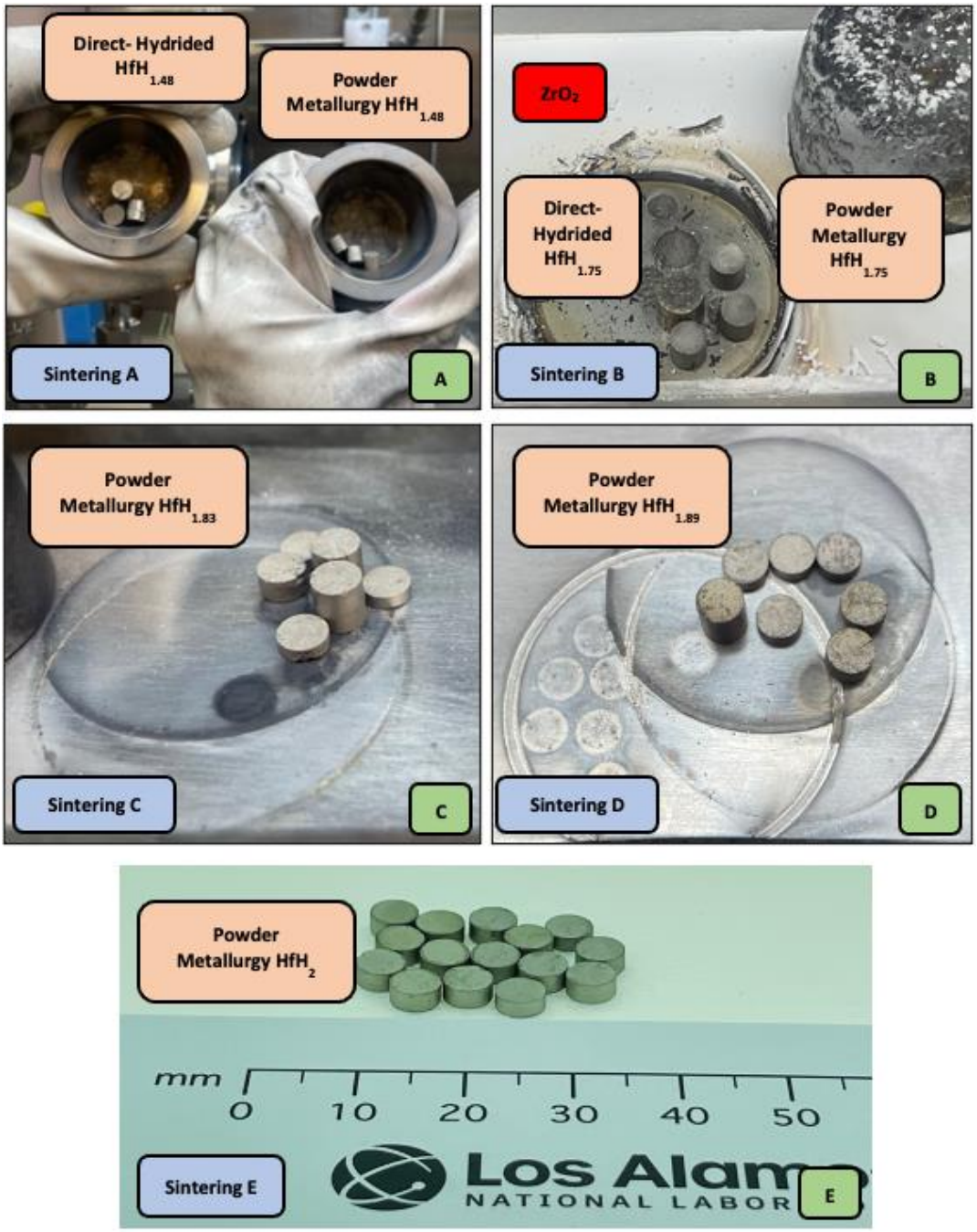

Figure 3. (a) Direct hydrided and powder metallurgy $HfH_{1.48}$ pellets produced from the Sintering A run. (b) Direct hydrided and powder metallurgy $HfH_{1.75}$ pellets produced from the Sintering B run. XRD results showed that the white powder was ZrO_2. (c) Powder metallurgy $HfH_{1.83}$ pellets of varying sizes produced from the Sintering C run. (d) Powder metallurgy $HfH_{1.89}$ pellets for thermophysical and microstructural analysis produced from the Sintering D run. (e) Powder

metallurgy HfH_2 pellets for the irradiation analysis produced from the second round Sintering E runs.

Inert Gas Fusion (IGF) was performed on the Sintering C, D and E samples using a LECO ONH836 elemental analyzer to confirm the H/Hf ratio calculated by weight. This method is sensitive to hydrogen and measures the hydrogen off gas from the combusted material. The H/Hf ratio is then calculated using the sample weights provided for testing. The results, shown in Table 2, confirm the increase in hydrogen concentration is correlated to the increase in hafnium-hydrogen ratio.

Table 2. LECO analysis summarized.

Sintering Temperature	Hydrogen %	H/Hf
Sintering B	0.978	1.75
Sintering C	1.02	1.83
Sintering D	1.05	1.89
Sintering E for Irradiation Batch 1	1.13	2.0
Sintering Efor Irradiation Batch 2	1.13	2.0

Microscopy was also performed on the Sintering A and Sintering D sintered samples to confirm density calculations through image analysis, shown in Figure 4. Prior to microscopy, the samples were ground until flat at 400 grit, and then ground approximately one minute at both 600 and 800 grit. The samples were then ground further for 45 seconds at 6μm, and finally for 30 seconds at 3μm. The samples were then put on a Buehler Vibromet for approximately 4 hours with no additional weight for final polishing.

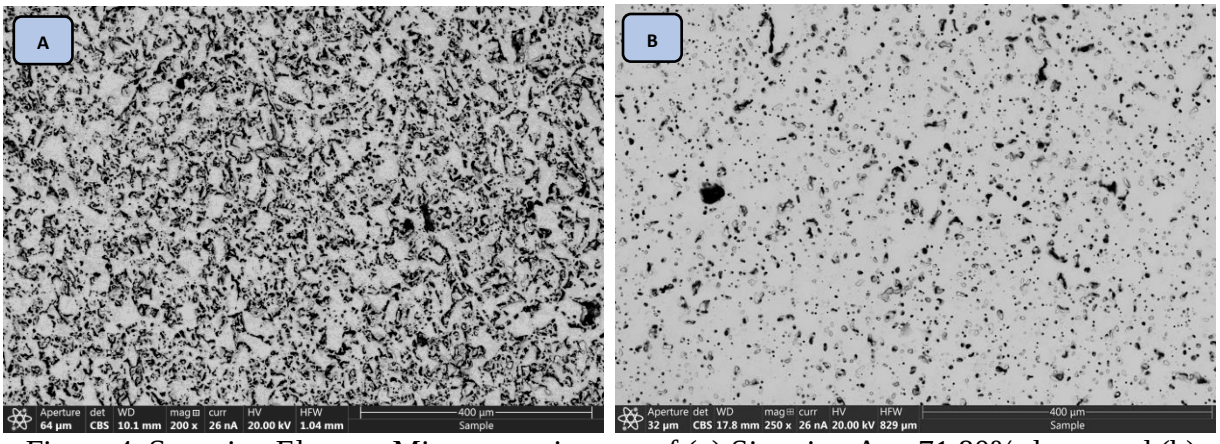

Figure 4. Scanning Electron Microscopy images of (a) Sintering A at 71.80% dense and (b) Sintering D sample at 90.91% dense.

Hydrogen desorption as a function of temperature was measured using a Netzsch simultaneous thermal analyzer (STA) Model 449 F3 Jupiter. This analysis method measures mass change from thermal effects, which in these samples is assumed to be the desorption of hydrogen. Samples were heated to approximately 1100 K at a ramp rate of 1 K/min under argon purge gas and mass

was recorded every 4 seconds. The results of this analysis, shown in Figure 5, are compared to a direct hydrided (100% dense) sample of the same Hf/H ratio of 1.89 and indicate that the powder metallurgy sample has a slightly different desorption rate. The STA results show that the powder metallurgy sample remains in the epsilon phase up to a higher temperature (~415°C), however, as both samples transition to the $\alpha + \delta$ phase the desorption rates begin to converge.

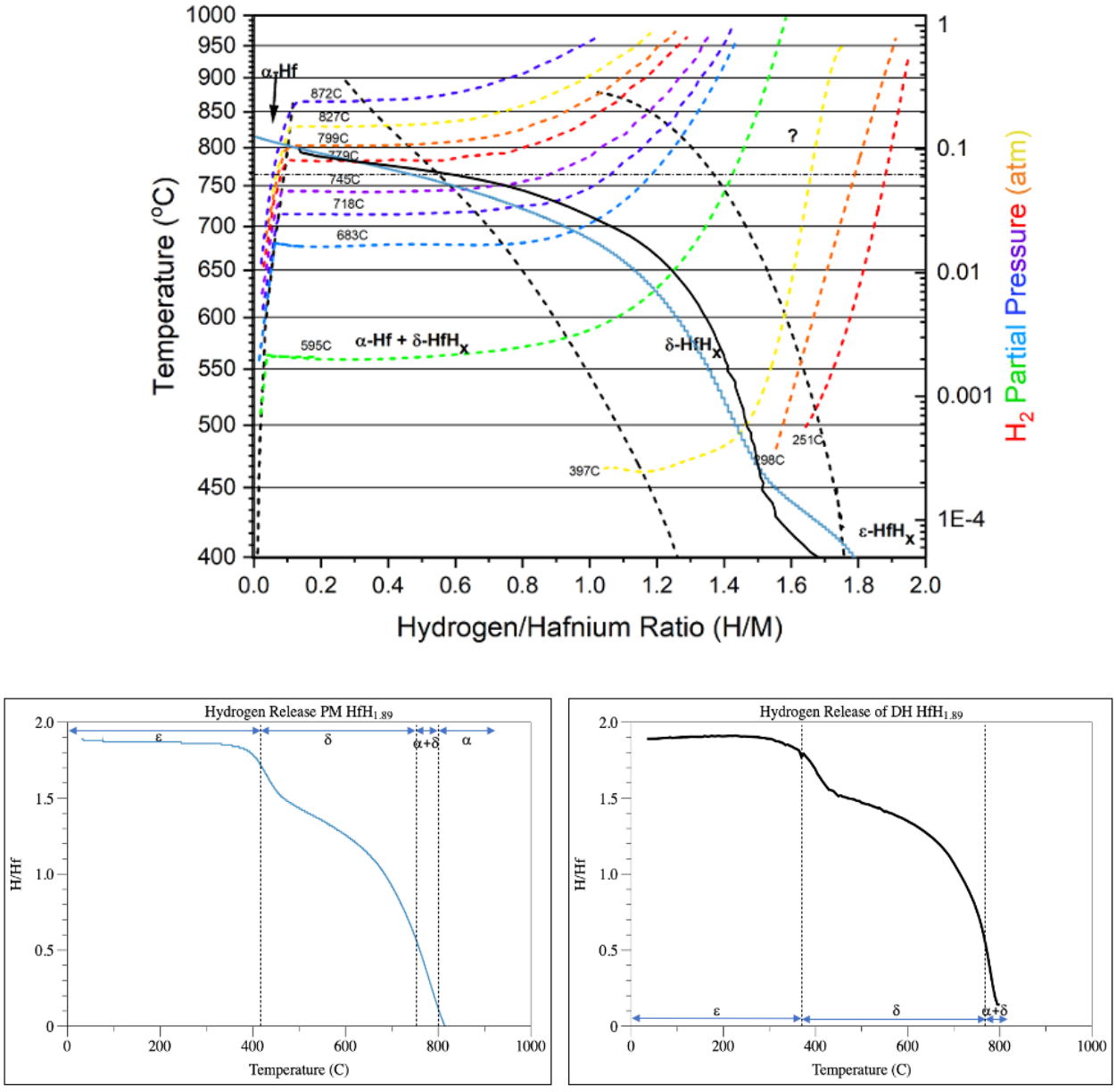

Figure 5. [Top] Dehydriding of Powder Metallurgy sample (blue) and Direct Hydrided sample (black) overlayed onto the H-Hf phase diagram to show expected phases for each sample during heat up. Both samples were $HfH_{1.89}$. [Bottom] STA Hydrogen Desorption profiles divided into expected phases for the powder metallurgy (left) and direct hydrided (right) samples.

Heat capacity measurements were acquired by differential scanning calorimetry (DSC) using a Netzsch DSC Model 404 F1 Pegasus. Each sample was calibrated using a 1 mm thick sapphire disc that was placed in an alumina-lined platinum crucible and covered with a platinum top cap. An argon cover gas was used to prevent oxidation during measurement exposure. Heat capacity measurements were acquired in the temperature ranges of 30°C to 600°C in 5°C increments. As seen in Figure 6, the heat capacity rose at a consistent rate within the epsilon phase (up to 330°C). However, as the sample changes from epsilon phase to delta phase at higher temperature, a Bredig transition was observed. According to the work of Bredig and Dworkin, this diffuse phase transition has been observed in FCC crystal structures [7], but thus far has not been observed in HfH_x until this project The effect of this transition can also be correlated to the phenomenon observed in the phase diagram of Figure 6. At 450°C the rate of hydrogen desorption slows as temperature increases, and the dissolution of hydrogen atoms within the hydrides are presumably able to restructure within the sample without desorbing.

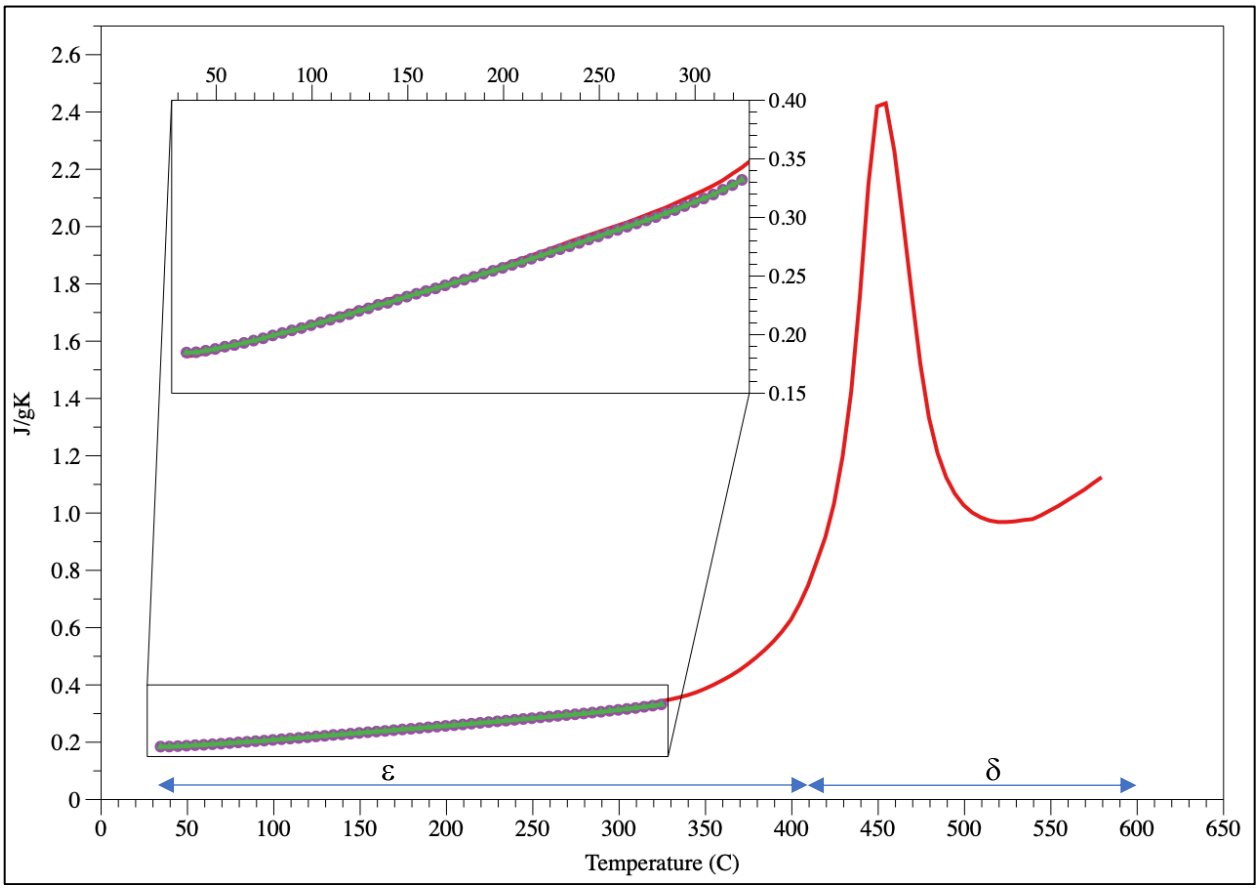

Figure 6. Heat capacity of $HfH_{1.89}$ measured by DSC. Consistent increase of heat capacity within the epsilon phase (shown in green, purple, and red), and a Bredig transition (red) is shown in the delta phase at higher temperatures.

Nanoindentation tests were performed on the $HfH_{1.89}$ samples with a Keysight G200 Nanoindenter using a diamond Berkovich tip to a final displacement of 400 nm with a constant strain rate of 0.05 s^{-1}. Continuous stiffness measurements (CSM) were applied at a frequency of

45 Hz with 2 nm displacement amplitude. Hardness measurements were determined using the Oliver-Pharr method. The hardness values are averaged at a depth region 200 - 400 nm below the surface to minimize the size effects from the strain gradient and are measured to be 4.45±1.63 GPa, as shown in Figure 7. The average value is consistent with the literature.

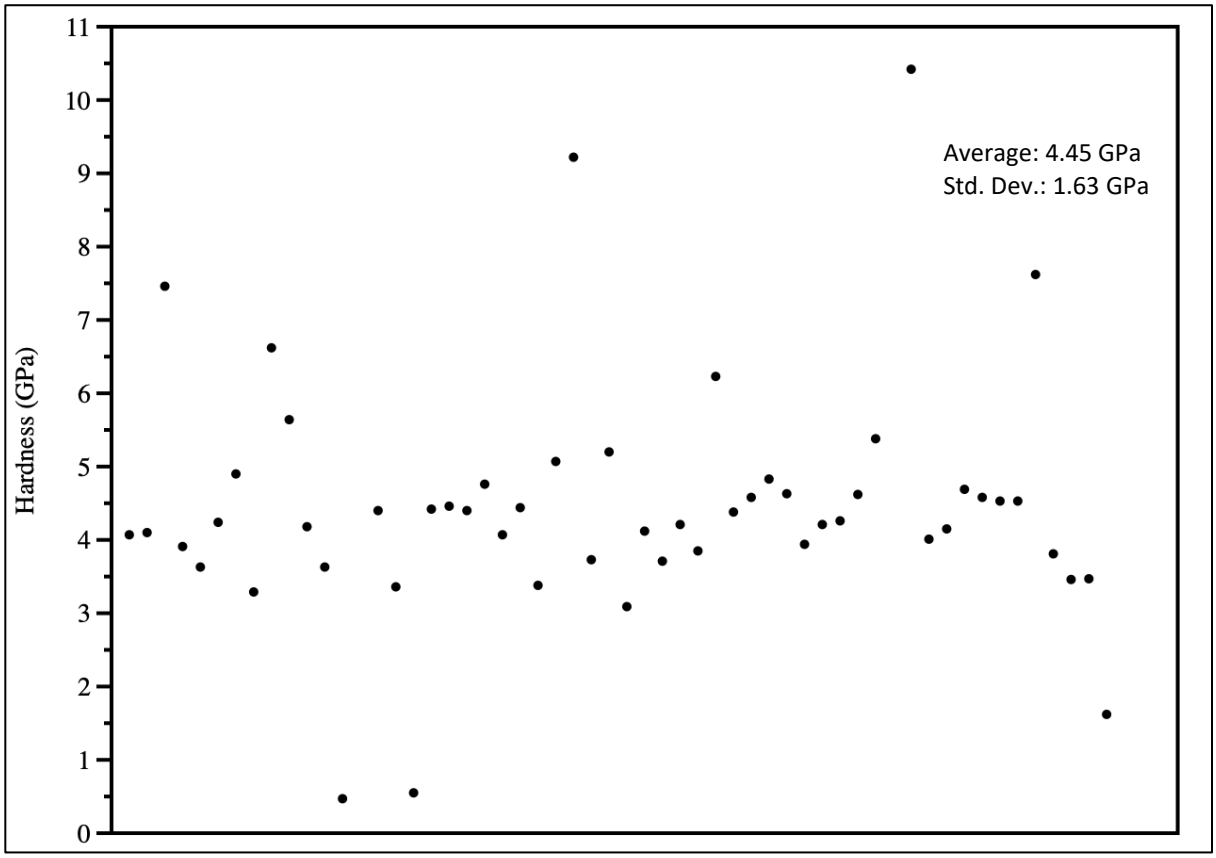

Figure 7. Hardness values of powder metallurgy Sintering D $HfH_{1.89}$.

2 Impact

2.1 Use of Project results

The powder metallurgy route has the potential to use feedstock powder of HfHx, rather than metallic Hf. This project results have shown that this manufacturing route is feasible by using optimal sintering routes (Sintering E parameters), producing HfH1.89 with a density of 90.46 – 90.91% whilst being crack free. The project results will be used for the next phase of the program, which will investigate the irradiation damage properties when exposed to neutron and ions to better understand the decomposition nature under these conditions.

2.2 Fusion Energy Impact

This project has demonstrated a means to fabricate a metal-hydride with excellent neutron and gamma shielding properties. A credible supply chain of Hf-H would greatly increase the attainable efficiency of the central column radiation shield in STs, which would substantially improve the

economic viability of a commercial reactor. A more efficient radiation shield would: a) reduce the overall volume (cost) of shielding materials, b) reduce the total length of HTS tape required, c) lower the radiation heating to HTS to fusion power ratio (Qrad/Pfus) enabling the tokamak to achieve higher Pfus for a given heating power, d) reduce the size, complexity and capacity of the necessary cryogenic plant, e) increase the HTS lifetime, and f) reduce the volume of radiation waste generated.

These characteristics and success of the project has given confidence in the upscale manufacturing needed in order to include such materials with a central column of a demonstration fusion power station (and eventually a commercial fusion power station).

References

[1] B. Tsuchiya, M. Teshigawara, K. Konashi, S. Nagata and T. Shikama, J. Alloys Compd., 446-447 (2007) 439.

[2] Sidhu S.S., McGuire J.C.: *An X-ray diffraction study of the hafnium-hydrogen system*. Journal of Applied Physics **23** (1952) 1257-1261

[3] Markin V.Y., Savin V.I.: *Temperature dependence of the magnetic susceptibility of hafnium hydrides*. Inorganic Materials (translated from Neorganicheskie Materialy) **19** (1983) 434-436

[4] Sidhu S.S.: *The Effect on Metal-Metal Bonds of Increased Concentration of Hydrogen in Hafnium Dihydride*. Acta Crystallographica **7** (1954) 447-449

[5] Dolukhanyan S.K.: *Synthesis of novel compounds by hydrogen combustion*. Journal of Alloys and Compounds **253/254** (1997) 10-12

[6] Artem V. Lunev, Boris A. Tarasov, A classical molecular dynamics study of the correlation between the Bredig transition and thermal conductivity of stoichiometric uranium dioxide, Journal of Nuclear Materials, Volume 415, Issue 2, 2011, Pages 217-221, ISSN 0022-3115